

## MODE CROSS-OVER AND DUCTILITY OF DOWELLED LVL AND CLT CONNECTIONS UNDER MONOTONIC AND CYCLIC LOADING

Lisa-Mareike Ottenhaus<sup>1</sup>, Minghao Li<sup>2</sup>, Tobias Smith<sup>3</sup>, Pierre Quenneville<sup>4</sup>

1 **ABSTRACT:** This paper presents an experimental study on dowelled connections in Cross-  
2 Laminated Timber (CLT) and Laminated Veneer Lumber (LVL) using  $\phi 20$  mm mild steel dowels  
3 and internal steel plates. Connections designed to fail in brittle row shear and group tear-out were  
4 tested under monotonic loading to assess the validity of analytical models from literature and code  
5 provisions. Connections designed to provide non-linearity before failure and thus produce ductility  
6 were tested under both monotonic and cyclic loading to study the influence of cyclic loading on  
7 ductility and the possibility of mode cross-over. It was found that cross layers in CLT improve  
8 ductility. Furthermore, mode cross-over from ductile response to brittle failure was observed in  
9 both CLT and LVL connections. Nevertheless, a good amount of ductility was achieved in all  
10 layouts (except the LVL connections designed for group tear-out failure) before cross-over to  
11 brittle failure occurred.

12 **KEYWORDS:** Dowelled connections, Cross-laminated timber, Laminated veneer lumber, Ductility,  
13 Cyclic loading, mixed-mode failure, mode cross-over

14

<sup>1</sup> Ph.D. Candidate, Department of Civil and Natural Resources Engineering, University of Canterbury, New Zealand, lisa-mareike.ottenhaus@pg.canterbury.ac.nz;

<sup>2</sup> Senior Lecturer, Department of Civil and Natural Resources Engineering, University of Canterbury, New Zealand, minghao.li@canterbury.ac.nz;

<sup>3</sup> Post-doc Research Fellow, Department of Civil and Natural Resources Engineering, University of Canterbury, New Zealand, tobias.smith@canterbury.ac.nz;

<sup>4</sup> Professor, Department of Civil and Environmental Engineering, University of Auckland, New Zealand, p.quenneville@auckland.ac.nz

## 15 **INTRODUCTION**

16 Traditionally, in timber buildings, connections provide the main source of non-linearity and energy  
17 dissipation during a seismic event because timber itself is prone to brittle failure. Therefore,  
18 connection behaviour needs to be well understood to ensure seismic safety of timber buildings.

## 19 ***DUCTILITY***

20 A building's ductile capacity is an important seismic design factor. Ductility is a measure of  
21 connection non-linearity and is commonly defined as  $\mu = \Delta_u / \Delta_y$ , where  $\Delta_y$  is the yield displacement  
22 and  $\Delta_u$  is the ultimate displacement, often defined as the post-peak displacement at 80% of the  
23 maximum load. Based on the assigned building ductility, the designer needs to detail specific  
24 connections with adequate ductility to achieve the desired reduction of seismic demand. This can  
25 be a challenging task, as it can be difficult to accurately predict the behaviour of connections under  
26 seismic loading. Furthermore, design codes often use ductility obtained from monotonic testing  
27 based on the assumption that similar ductile behaviour can be achieved under cyclic loading (Smith  
28 et al. 2015, Ottenhaus et al. 2016). In addition, it should be noted that different definitions of the  
29 yield point can lead to inconsistencies of ductility evaluations unless clearly defined in design  
30 codes (Jorissen and Fragiaco 2011, Piazza et al. 2011, Flatscher 2016). For the purpose of this  
31 paper a connection which has a clearly defined yield point establishing non-linear behaviour is  
32 considered to be responding in a ductile manner.

## 33 ***MODE CROSS-OVER***

34 Ductile and brittle behaviour of dowel-type connections have been extensively studied in literature  
35 (Jorissen and Fragiaco 2011, Piazza et al. 2011, Quenneville and Morris 2009, Jensen and  
36 Quenneville 2011). Traditionally, ductile and brittle modes are treated as two separate responses.  
37 It is assumed that brittle failure can be avoided with adequate fastener spacing allowing the

38 connection to develop sufficient ductility. However, fastener embedment and associated timber  
39 densification underneath the fastener can reduce the effective shear plane length of the brittle  
40 modes and thereby decrease the connection's resistance against brittle failure (Novis et al. 2016,  
41 Zhang et al. 2016). A previously ductile responding connection can thus 'cross-over' to brittle  
42 failure which is referred to as mixed-mode response.

43 Fig. 1 shows the theoretical concept of cross-over:  $F_{BRu}$  refers to the connection's theoretical  
44 ultimate brittle resistance. For dowelled connections,  $F_{BRu}$  can be the ultimate row shear strength,  
45  $F_{RSu}$ , the ultimate group tear-out strength,  $F_{GTu}$ , or the ultimate net tensile strength,  $F_{NTu}$ . The  
46 respective brittle failure modes are displayed in Fig. 2a. As  $F_{NTu}$  is not affected by dowel  
47 embedment it can be excluded in this illustration.  $F_{EYMu}$  denotes the connection's theoretical  
48 ultimate ductile capacity according to the European Yield Model (EYM) as shown Fig. 2b.  $F_{EYMy}$   
49 is reached at the displacement  $\Delta_y$  and is the connection's yield strength,  $F_y$ , regardless of the  
50 ultimate failure mode.  $F_u$  is the obtained ultimate strength at the displacement  $\Delta_u$ . Note that  $F_u$  is  
51 defined as 80%  $F_{max}$ , however, if brittle failure occurs,  $F_u$  and  $F_{max}$  and the corresponding  
52 displacements are identical.

53 Fig. 1 shows the different possible connection responses which are defined by the connection's  
54 strength hierarchy:

55 a) Ductile: If  $F_{BRu} \gg F_{EYMu}$ , the connection is able to respond in a fully ductile manner as  $F_u$   
56  $= F_{EYMu}$

57 b) Ductile mixed-mode: If  $F_{BRu}$  is higher than  $F_{EYMu}$ , mode cross-over occurs before  $F_{EYMu}$  is  
58 reached:  $F_u < F_{EYMu}$ . However, the connection may still be able to achieve a high level of  
59 ductility depending on the initial difference between  $F_u$  and  $F_{EYMy}$  and accordingly the  
60 difference between  $\Delta_u$  and  $\Delta_y$ .

61 c) Nominally ductile mixed-mode: If the strength hierarchy of the connection is  $F_{EYMy} < F_{BRu}$   
62  $< F_{EYMu}$ , only a small amount of non-linear deformation can be achieved before mode cross-  
63 over occurs resulting in a connection with nominal ductility.

64 d) Brittle: If  $F_{BRu} < F_{EYMy} < F_{EYMu}$ , the connection will fail without any fastener yielding.

65

66 If the connection's ductile behaviour is well described and the expression for the reduced brittle  
67 strength,  $F_{BRred}$ , is known, it is possible to accurately predict  $\Delta_u$  and the connection's ductility  
68  $\mu = \Delta_u / \Delta_y$  (Zhang et al. 2016, Novis et al. 2016), without conducting experimental testing.

69

70 The effect of cyclic loading on strength and ductility has been studied in literature (Mohammad et  
71 al. 1998, Yasumura 1998). As fastener embedment can only provide limited hysteretic energy  
72 release under cyclic loading, timber structures rely on fastener yielding for ductility during seismic  
73 events. However, this ductile response can be impaired by onset of brittle failure due to mode  
74 cross-over.

75

## 76 **EXPERIMENTS**

77 Monotonic and cyclic tensile tests were performed on dowelled connections in Laminated Veneer  
78 Lumber (LVL) and Cross-Laminated Timber (CLT) made out of New Zealand *Radiata pine*. The  
79 connection layouts, based on Eurocode 5 provisions (EN 1995-1-1 2004) and models developed  
80 by Quenneville and Morris (2009), were designed to result in ductile and brittle responses with  
81 little margin between the different failure modes. Subsequently, the accuracy of the strength  
82 prediction and the mode cross-over was assessed. One connection layout was additionally

83 subjected to cyclic loading according to ISO 16670 (2003) to study the effects of cyclic loading  
84 on strength, ductility and mode cross-over.

85

## 86 ***TEST SET-UP AND MATERIALS***

87 As shown in Fig. 3a, all CLT and LVL connection specimens were 610 mm long and 240 mm  
88 wide with a 20 mm slot to insert a 20 mm thick Grade 300 steel plate. The LVL specimens were  
89 133 mm thick with a side member thickness of  $t_l = 56.5$  mm. The CLT specimens were 130 mm  
90 thick with a side member thickness of  $t_l = 55$  mm. The outer layers were 35 mm thick, whereas the  
91 cross-layers and inner layer were 20 mm thick.

92 The LVL specimens were grade LVL13 with a manufacturer specified Modulus of Elasticity  
93 (MOE) value of 13.2 GPa and a measured average moisture content of 8.4%. The veneers in the  
94 LVL specimens were 2.5 - 4.4 mm thick and glued with phenolic adhesive complying with  
95 AS/NZS 4357.0 (2005). The mean and characteristic (5<sup>th</sup>-percentile) densities were  $\rho_{mean}$   
96  $= 591 \text{ kg/m}^3$  and  $\rho_k = 585 \text{ kg/m}^3$ , respectively.

97 The CLT connection specimens had an average moisture content of 9.9%. Timber lamellas in the  
98 CLT specimens were 120 mm wide and glued with single-component polyurethane adhesive  
99 (PUR) without edge-gluing. The average MOE of the lamellas was 8 GPa in the outer layers and  
100 6 GPa in the inner layers. The mean and characteristic density were  $\rho_{mean} = 443 \text{ kg/m}^3$  and  $\rho_k =$   
101  $412 \text{ kg/m}^3$ , respectively.

102 As shown in Fig. 3b, the top connection joining to the loading head was designed to be  
103 significantly stronger than the bottom connection subjected to destructive testing and consisted of  
104 six  $\phi 25$  mm Grade 300 dowels reinforced with self-tapping screws. The bottom connection  
105 consisted of four chamfered  $\phi 20$  mm dowels that were flush with the timber surface and were

106 sourced from the same batch as those tested in dowel bending and embedment. The connection  
107 was designed as described in the following section with different layouts targeting three different  
108 strength hierarchies in LVL, depending on the fasteners spacing  $a_1$  and  $a_2$ , and the end distance  $a_3$   
109 and the edge distance  $a_4$  as shown in Fig. 3c and Table 1:

- 110 - brittle row shear failure (RS) under monotonic loading  $F_{EYMy} < F_{RSu} < F_{EYMu}$
- 111 - brittle group tear out failure (GT) under monotonic loading  $F_{GTu} < F_{EYMy} < F_{EYMu}$
- 112 - ductile response under monotonic (DT-M) and cyclic (DT-C) loading  $F_{EYMy} < F_{EYMu} < F_{BRu}$

113 The same layouts were adopted for the CLT specimens to study the reinforcing effect of the cross  
114 layers depending on the connection layout. It should be noted that the designations RS, GT, DT  
115 refer to the connection layout rather than the observed actual response from experimental testing.  
116 Five connection replicates for each layout were tested with a loading rate of 1 mm/s under  
117 monotonic loading and 10 mm/s under cyclic loading. The cyclic tests followed the ISO loading  
118 protocol (ISO 16670 2003), with the specimens being loaded to the target displacement of each  
119 cycle group and then returned to zero displacement. Each cycle group consisted of three repeated  
120 cycles whose target displacement was a certain percentage of the average  $\Delta_u$  obtained from the  
121 monotonic tests. This was to represent a typical hold-down connection subjected to repeated  
122 uplifting in a seismic event. Displacements were measured with potentiometers at six different  
123 locations (front, back, two locations on each side) and averaged.

124

## 125 ***STRENGTH PREDICTION***

126 Table 2 lists the characteristic strength properties of CLT, LVL, and the fasteners that served to  
127 calculate the connection's nominal strength, taken as the 5<sup>th</sup>-percentile value of the strength  
128 distribution. All strength predictions were based on measured material properties rather than

129 supplier specified properties with the exception of the characteristic shear strength,  $f_{v,k}$ , and  
130 characteristic tensile strength,  $f_{t,k}$ , which were provided by the CLT and LVL manufacturers.

131 As embedment strength values for CLT were not available, additional CLT embedment tests were  
132 performed according to AS/NZS ISO 10984.2 (2015) and the characteristic embedment yield  
133 strength,  $f_{h,y,k}$ , was determined from the load-deformation graphs according to EN 12512 (2013).

134 The relationship  $f_{h,y,k} \approx 0.8 f_{h,u,k}$  was established with  $f_{h,u,k}$  being the characteristic ultimate  
135 embedment strength (Ottenhaus et al. 2017). The characteristic embedment strength for the LVL  
136 specimens was calculated according to Franke and Quenneville (2011) as  
137  $f_{h,u,k} = 0.075(1 - 0.0037d) \rho_k$ . Furthermore, three-point dowel bending tests were performed  
138 according to AS/NZS ISO 10984.1 (2015) and the plastic yield moment was determined as  
139  $M_{y,p} = 428,700 \text{ Nmm}$  from which the elastic yield moment was calculated as  $M_{e,p} = (6\pi/32) M_{y,p}$   
140 (Ottenhaus et al. 2017).

141

142 The ductile strength prediction was based on the European Yield Model (EYM) as presented in  
143 Eurocode 5 (EN 1995-1-1 2004). An attempt was made not only to predict the connection's  
144 characteristic maximum capacity  $F_{max,k}$  (equivalent to  $F_{v,Rk}$ , in Eurocode 5), but also to predict the  
145 characteristic yield strength,  $F_{y,k}$ . The governing ductile mode was EYM VI (see Fig 2b). The  
146 corresponding ductile capacity was calculated using Equations (1) and (2), simply referred to as  
147  $F_{EYM_y}$  and  $F_{EYM_u}$  in the following context.

148

149 The brittle strength prediction for LVL was adopted from Quenneville and Morris (2009) and  
150 conservatively modified for accuracy, as shown in Equation (3) and (4). The calibration factors  $\alpha_i$   
151 were adopted from Quenneville and Morris (2009). Currently, no expressions for the reduced

152 brittle strength due to dowel embedment,  $RS_{red}$  and  $GT_{red}$ , exist (Zhang et al. 2016). Therefore, it  
 153 was unlikely to accurately represent the impact of this phenomenon on the brittle failure prediction.

$$F_{EYM_{y,k}} = 4 \times 2 f_{h,y,k} t_1 d \left( \sqrt{2 + \frac{4M_{y,e,k}}{f_{h,e,k} d t_1^2}} - 1 \right) \quad (1)$$

$$F_{EYM_{u,k}} = 4 \times 2 f_{h,u,k} t_1 d \left( \sqrt{2 + \frac{4M_{y,p,k}}{f_{h,u,k} d t_1^2}} - 1 \right) \quad (2)$$

$$F_{RS_{u,k}} = 2n_2 \times \alpha_1 f_{v,k} k_{LS} (n_1 \min[a_1; a_3] - d) 2t_1 \quad (3)$$

$$F_{GT_{u,k}} = 2 \times \alpha_1 f_{v,k} k_{LS} (n_1 \min[a_1; a_3] - d) 2t_1 + \alpha_2 f_{t,k} (n_2 - 1)(a_2 - d) 2t_1 \quad (4)$$

154 where  $k_{LS}$  = loading surface factor (0.65 for internal steel plate),  $\alpha_1$  = row shear calibration factor  
 155 (0.84),  $\alpha_2$  = group tear-out calibration factor (1.26),  $a_i$  = fastener spacing (shown in Fig. 3c),  $d$  =  
 156 fastener diameter,  $t_1$  = single side timber thickness.

157 Table 3 gives the predicted connection strength values based on Equation (1) through Equation (4).  
 158 Currently, there are no brittle strength predictions available for the CLT connections due to the  
 159 crosswise layup of lamellas. However, the aim was to study the reinforcing effect of the cross-  
 160 layers depending on different connection layouts. Therefore, the CLT specimen layouts were based  
 161 on the LVL and the designations RS and GT were adopted for consistency.

162

### 163 **EXPERIMENTAL RESULTS OF CLT CONNECTIONS**

164 The CLT connections had 3-stages of response before failure:

165 1) Onset of dowel bending and yielding (Fig. 4a);

166 2) Continued yielding, out-of-plane bending of the timber members and onset of crack growth  
167 in cross layers (Fig. 4b). Shear failure in cross layer and separation of outer layer and cross  
168 layer close to the glue line;

169 3) Final brittle rupture in the outer layers (Fig. 4c and d).

170 Development of the second stage was influenced by the position of lamella edges in the outer  
171 layers and inherent imperfections such as knots and initial cracks. Furthermore, out-of-plane  
172 bending of the timber members and separation of the cross layer from the outer layer often caused  
173 premature brittle failure (Fig. 4e). The yield strength,  $F_y$ , of the load-displacement curves was  
174 defined according to EN 12512 (2013) with correction of some initial slip. This method was  
175 deemed appropriate as it does not produce a yield point for brittle behaviour (Brühl et al. 2011).

176

177 **Table** Tables 4 and 5 display the yield strength,  $F_y$ , maximum strength,  $F_{max}$ , strength at failure,  
178  $F_u$ , initial stiffness,  $K$ , and the corresponding displacements  $\Delta_y$ ,  $\Delta_{Fmax}$ , and  $\Delta_u$ . The ductility was  
179 calculated as  $\mu = \Delta_u / \Delta_y$  and the failure mode as well as the ductility classification were adopted  
180 from Smith et al. (2006):  $\mu \leq 4$  brittle/low ductility (B),  $4 < \mu \leq 6$  mixed (M),  $\mu > 6$  ductile (D).  
181 The load-displacement curves and the strength predictions are shown in Fig. 5 and Fig. 6.  
182 The load-displacement hysteretic curves for the DT-C specimens are shown in Fig. 7. It should be  
183 noted that RS01 and RS04 displayed high ductility as  $\Delta_y$  was very small compared to  $\Delta_{Fmax}$  and  
184  $\Delta_u$ . This would not be the case if another method such as Energy Equivalent Elastic Plastic (EEEP)  
185 method was used to establish  $\Delta_y$  (Jorissen and Fragiacommo 2011, Brühl et al. 2011, Piazza et al.  
186 2011). Another option to quantify ductility in a more meaningful manner is to use a combination  
187 of relative and absolute ductility definitions that can potentially also avoid the determination of  
188 the yield point as suggested by Flatscher (2016).

189

## 190 ***EXPERIMENTAL RESULTS OF LVL CONNECTIONS***

191 For the LVL connection specimens, all DT-M, DT-C and RS specimens ultimately failed in row  
192 shear or tensile splitting with significant dowel yielding in bending. The GT specimens developed  
193 the expected group tear-out with little dowel bending (Fig. 8).

194 Tables 6 and 7 list the yield strength,  $F_y$ , peak strength,  $F_{max}$ , ultimate strength,  $F_u$ , initial stiffness,  
195  $K$ , and the corresponding displacements  $\Delta_y$ ,  $\Delta_{Fmax}$ ,  $\Delta_u$ . The yield point, failure mode and ductility  
196 were established with the same methods as for the CLT connections. The load displacement curves  
197 and strength predictions are displayed in Fig. 9 and 10. The hysteretic curves for the DT-C  
198 specimens are shown in Fig. 11.

199

## 200 **DISCUSSION**

201 The test results showed that the CLT and LVL connections with  $\phi 20$  mm dowels can be designed  
202 to achieve good ductility (on average 6.2 – 14.6 from the ductile responses) and ultimate  
203 displacement capacity even if the connection is eventually governed by the mixed-mode response,  
204 as shown in Table 8. It should be emphasized that the achieved connection ductility does not equate  
205 system ductility or overall building ductility which requires the consideration of total building  
206 displacement (Moroder et al. 2014).

207

### 208 ***DUCTILITY IN CLT CONNECTIONS***

209 Non-glued edges and gaps in the crosswise CLT layup affected the strength and resulted in high  
210 scatter of the test results. Therefore, it could be beneficial to spread out fasteners over a wider  
211 connection area to engage more cross layers and prevent brittle failure. Low rolling shear strength  
212 of the cross layers can cause separation from the outer layers and lead to brittle failure as the  
213 smooth steel dowels are not able to prevent opening up of the side members. Further investigations  
214 should also examine the influence of fastener spacing, edge distances and location of lamella gaps  
215 on ductility and brittle failure modes through comprehensive experimental research and/or robust  
216 finite element modelling.

217 For the CLT connections, the RS layout achieved twice as much ductility at the DT layout, which  
218 indicated that the increase of the end distance  $a_3$  from  $5d$  to  $7d$  was very beneficial.

219

220 ***DUCTILITY IN LVL CONNECTIONS***

221 The LVL connections can achieve very high ductility if edge distances are increased such that  
222  $F_{BRred} > F_{EYMu}$ . However, this still requires quantification of the strength reduction,  $F_{BRk,red}$ , due to  
223 dowel embedment (Zhang et al. 2016).

224 The DT-M, DT-C layout and the RS layout achieved good ductility (average range of 6.2 – 9.8),  
225 whereas the GT layout failed before the onset of significant non-linear behaviour (average ductility  
226 of 2.5). The increase of edge distance  $a_3$  from DT to RS improved the ductility in the LVL  
227 connections, although the effective shear plane length was reduced from  $2 \cdot \min[a_1, a_3] - d =$   
228  $2 \cdot 100 - 20 = 180$  mm to  $2 \cdot 80 - 20 = 140$  mm.

229 If it is assumed that the initial stiffness,  $K$ , is independent of the connection layout, the yield  
230 displacement,  $\Delta_y$ , should be identical for all connection layouts as the EYM strength is independent  
231 of the connection layout ( $\Delta_y = F_{EYMy} / K$ ). As shown in Fig. 1, the DT layout should theoretically  
232 achieve a higher ultimate displacement,  $\Delta_u$ , than the RS layout before mixed-mode failure occurs.  
233 Consequently, the DT layout's ductility,  $\mu_{DT}$ , should be higher than the RS ductility,  $\mu_{RS}$ , and the  
234 following expression should hold:  $\mu_{DT} \geq \mu_{RS}$ .

235 However, for the LVL specimens, the observed ultimate displacements were  $\Delta_{u,DT} = 7.4$  mm and  
236  $\Delta_{u,RS} = 8.3$  mm, and the values for initial stiffness were  $K_{DT} = 144$  kN/mm and  $K_{RS} = 157$  kN/mm,  
237 which resulted in  $\mu_{RS} > \mu_{DT}$ . This finding suggests that the increased edge distances and fastener  
238 spacing might have an impact on the initial stiffness,  $K$ , and brittle strength reduction,  $F_{BR,red}$ . This  
239 issue should be further investigated.

240

241 ***CYCLIC AND MONOTONIC DUCTILITY***

242 The CLT and LVL connection specimens showed increased ductility under cyclic loading: cyclic  
243 ductility was 1.15 times larger than monotonic ductility for the CLT connections, and 1.58 times  
244 larger for the LVL connections. This finding is in agreement with previous observations by  
245 Mohammad et al. (1998) but contradicts findings by Yasumura (1998). Therefore, the difference  
246 between cyclic and monotonic ductility should be further investigated with a larger sample size  
247 taking different displacement rates and loading protocols into account.

248

249 ***MODE CROSS-OVER***

250 Table 8 compares the respective strength predictions ( $F_{EYM_y,k}$ ,  $F_{EYM_u,k}$ ,  $F_{BRu,k}$ ) to the experimentally  
251 obtained average maximum values.

252 Mixed-mode response was observed in the DT layouts and brittle failure occurred before the  
253 ultimate ductile capacity,  $F_{EYM_u}$ , was reached:  $F_{EYM_y} < F_u = F_{BRred} < F_{EYM_u} < F_{BRu}$ .

254 The strength predictions of the brittle layouts (GT and RS) in the LVL connections were  
255 conservative. Such conservatism is deemed appropriate due to the inherently high scatter in  
256 strength of brittle modes. However, too much conservatism should be avoided as it results in  
257 uneconomic designs.

258 It should be noted that the determination of  $F_y$  according to EN 12512 (2013) depends on the  
259 measured ultimate strength,  $F_u$ . Nevertheless, the prediction of  $F_y$  was fairly accurate for all the  
260 connection designs with the average error being within 10%. However, the error may be larger if  
261 all the supplier specified material properties were used for the strength predictions.

262 Ultimate and yield strength values achieved under cyclic loading were slightly higher than those  
263 under monotonic loading. As crack growth is dependent on time, this strength increase may be due

264 to the higher displacement rate under cyclic loading. However, this hypothesis should be verified  
265 further with a larger sample size for different displacement rates and loading protocols.

266

## 267 **CONCLUSIONS**

268 A total of 40 experimental tests were performed on dowelled CLT and LVL connections with three  
269 different layouts (ductile, row shear and group tear-out). Embedment tests on CLT and dowel  
270 bending tests were also performed to calibrate the input parameters for strength predictions of the  
271 connections.

272 The experimental results showed that the models for brittle failure (Quenneville and Morris 2009)  
273 were able to conservatively predict row shear failure and group tear-out failure in the LVL  
274 connection layouts. Given the high scatter in brittle modes, conservatism for brittle connection  
275 failure is deemed appropriate. However, better calibration of the model parameters could be  
276 performed to reduce some of this conservatism.

277 Purely ductile response ( $F_u = F_{EYMu}$ ) was not achieved in the monotonic or cyclic experiments of  
278 the LVL connections as dowel yielding through bending was followed by row shear. This was due  
279 to the fact that the connection capacity decreases as the effective shear plane length is reduced by  
280 dowel embedment and timber densification underneath the dowel (Zhang et al. 2016, Novis et al.  
281 2016). This mixed-mode response could not be reasonably predicted due to the lack of good  
282 prediction of the brittle strength reduction,  $F_{BRred}$ .

283 Brittle failure modes need to be further studied for dowelled CLT connections. Existing gaps in  
284 non-edge glued CLT can act as pre-existing shear failure planes which dramatically decrease  
285 connection strength and ductility. Low rolling shear strength of the cross layers may also lead to  
286 pre-mature failure which causes further strength reduction. However, if bolts were used as

287 fasteners, they could help prevent the out-of-plane bending and opening up of the side members  
288 in the connection. Nevertheless, there was an indication that the cross layers had a reinforcing  
289 effect for the CLT connections and good ductility (average ductility 7.3 – 14.6) was achieved if  
290 brittle failure was avoided.

291 Slightly higher yield and ultimate strength and slightly greater ductility were achieved under cyclic  
292 loading when compared to monotonic loading for both CLT and LVL connections (average of 8.4  
293 vs 7.3 for the CLT connections and 9.8 vs 9.1 for the LVL connections). This indicates that it is  
294 possible to represent the cyclic backbone curves by the monotonic curves in terms of strength and  
295 ductility for dowelled connections that respond in a ductile mixed-mode manner. However, further  
296 experimental testing with a larger sample size, different connection layouts, displacement rates,  
297 and loading protocols is required to confirm this finding. Furthermore, a test series with purely  
298 ductile response is required to extrapolate this finding to completely ductile connection layouts.

299 The test results suggest that good ductility (on average 7.3 - 14.6) can be achieved for dowelled  
300 connections in LVL and CLT even if mixed-mode response is ultimately governing, as long as the  
301 connection layout is configured such that the ultimate ductile strength based on the European Yield  
302 Model is lower than the ultimate brittle strength  $F_{EYMu} \leq F_{BRu}$ . Further increase in connection  
303 ductile capacity could be achieved if the strength hierarchy for purely ductile response is targeted:

$$304 \quad F_{EYMu} \leq F_{BRu,red}.$$

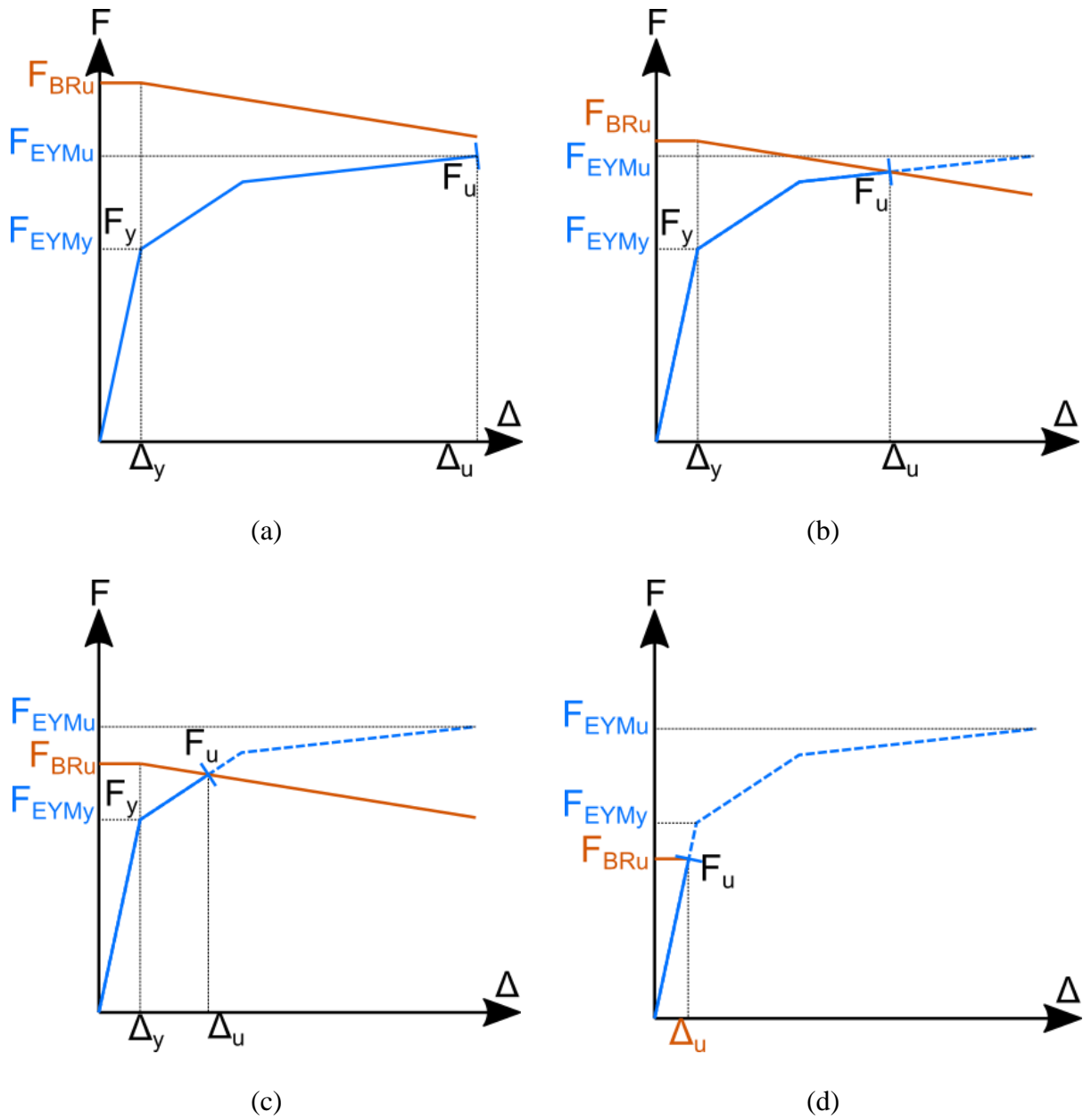
305 In this study, EN 12512 was used to define the yield point as it does not produce a yield point for  
306 brittle failure. However, when the initial stiffness is calculated between 10% and 40% of the  
307 maximum load, the established yield displacement,  $\Delta_y$ , can be very small which can lead to a  
308 misleadingly high ductility  $\mu$  in some cases. Critical evaluation of the yield point and ductility  
309 definitions is required to give more rational ductility estimations.

310

311 **ACKNOWLEDGEMENTS**

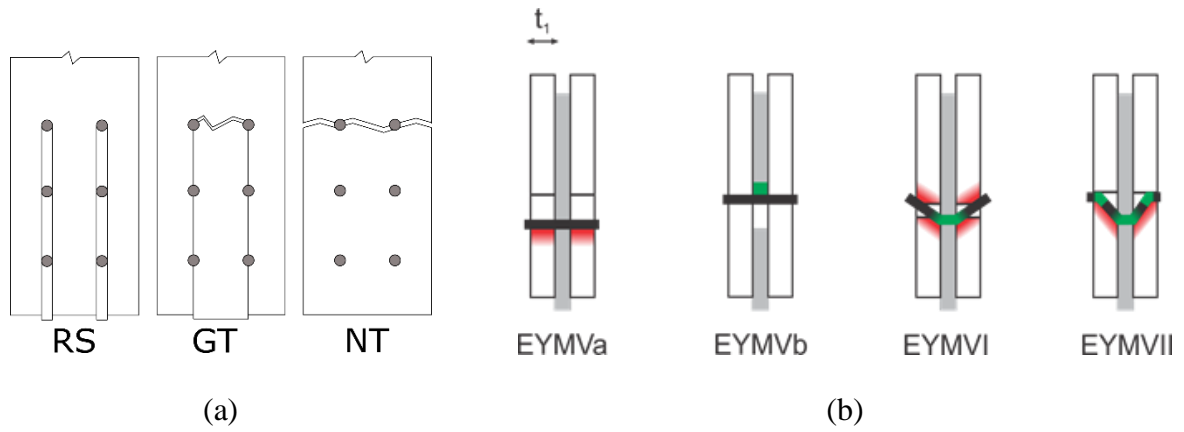
312 The authors would like to acknowledge Natural Hazard Research Platform of New Zealand and  
313 Department of Civil & Natural Resources Engineering at University of Canterbury for providing  
314 research funding. XLAM NZ Ltd. and Nelson Pine Industries Ltd. are also gratefully acknowledged  
315 for providing the test specimens. The authors would also like to thank Mr. Shane Magic and Mr.  
316 Jared McPherson for conducting the CLT embedment tests and Mr. Alan Poynter for providing  
317 technical laboratory assistance.

318

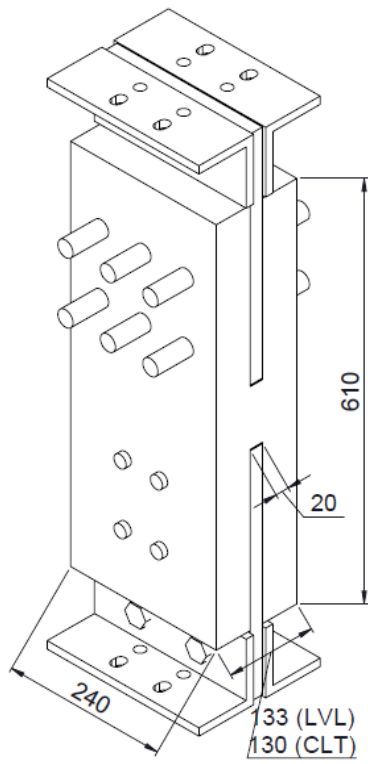


320 **Fig. 1.** Concept of mode cross-over from left to right: (a) Ductile, (b) ductile mixed-mode, (c) low  
 321 ductility mixed-mode, (d) brittle

322



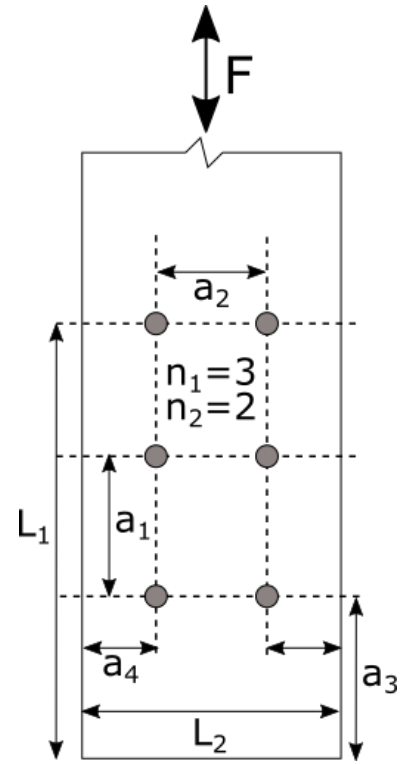
323 **Fig. 2.** (a) Brittle failure modes (Row Shear, Group tear-out, Net tensile failure) (b) Ductile  
 324 modes according to European Yield Model (red shows timber crushing, green shows steel  
 325 yielding)  
 326



(a)



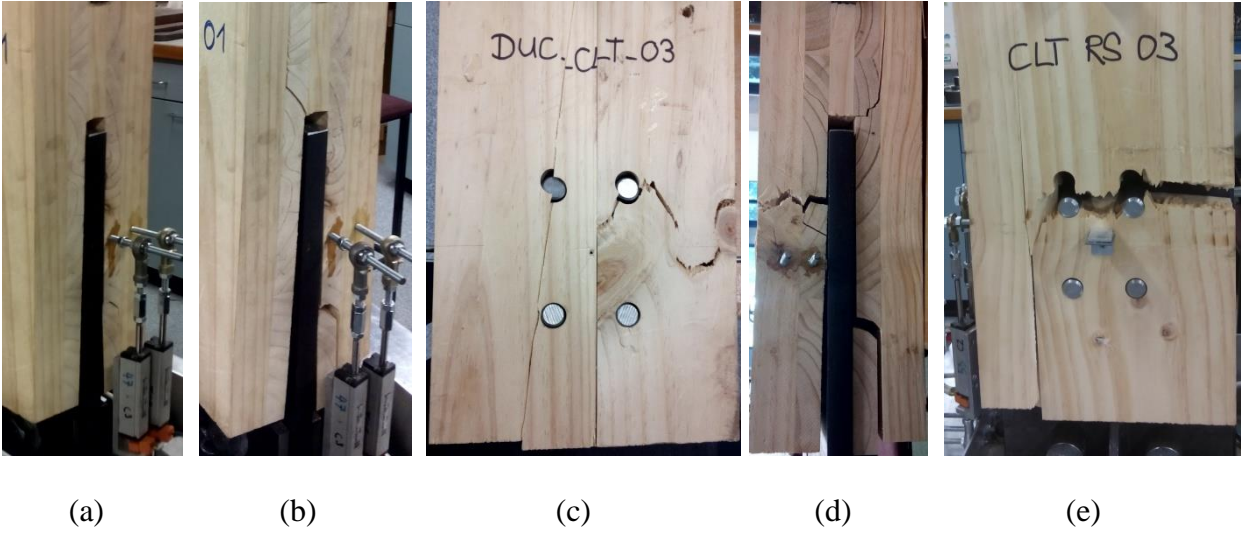
(b)



(c)

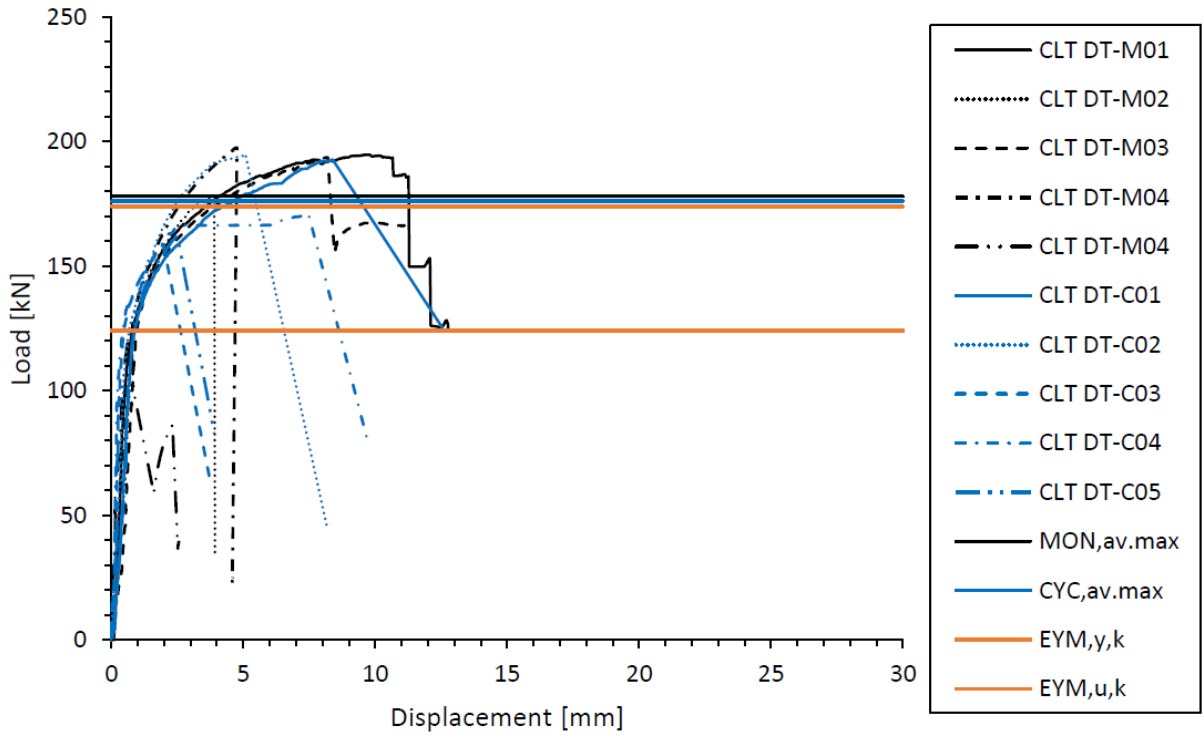
327 **Fig. 3.** (a) Layout and (b) set-up for monotonic and cyclic testing (c) fastener spacing

328



329 **Fig. 4.** Failure in CLT specimens from left to right: (a) onset of cracking in cross layer, (b) crack  
330 propagation, (c) DT layout failure front, (d) DT layout failure side, (e) RS layout failure  
331

CLT ductile monotonic (DT-M) and cyclic (DT-C) connection tests

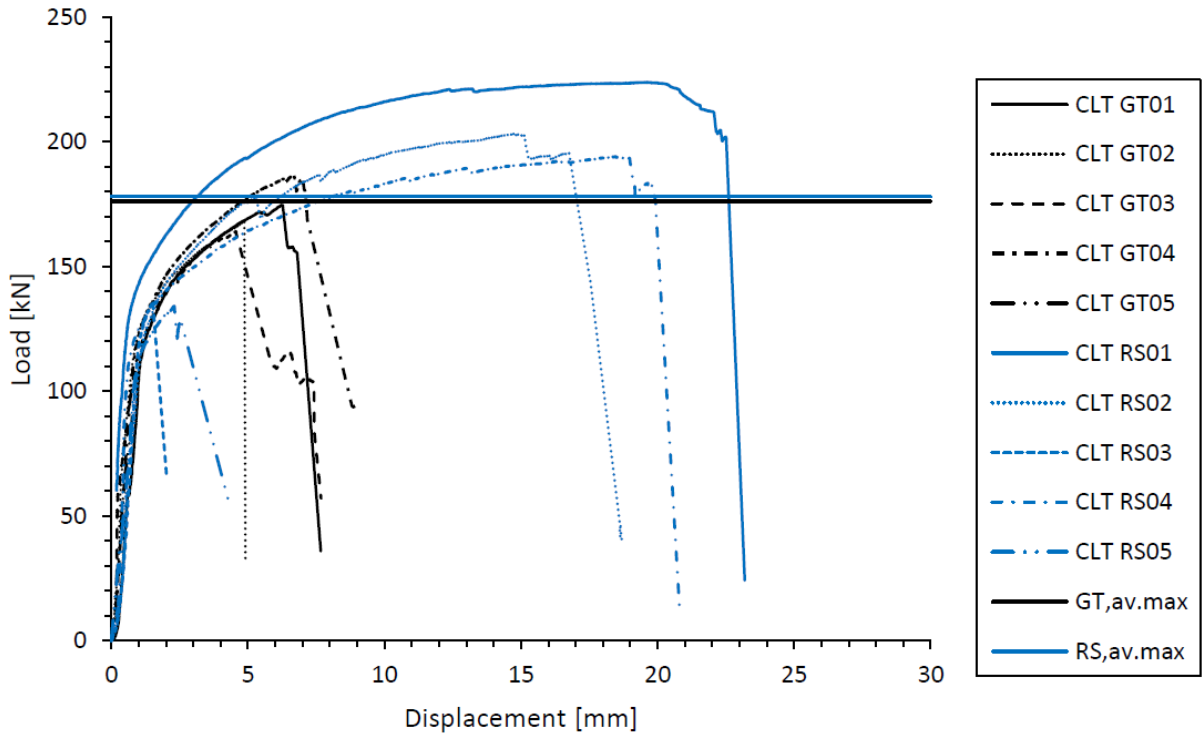


332

333 **Fig. 5.** Load displacement curves of CLT connections with ductile layout

334

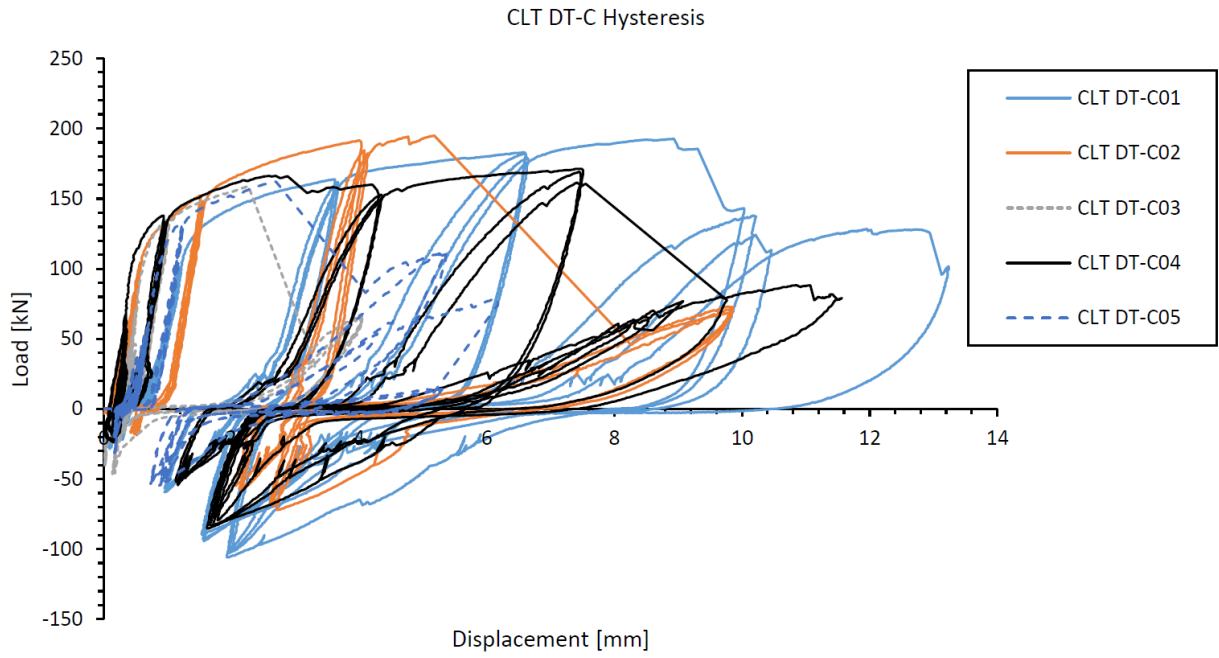
CLT group tear-out (GT) and row shear (RS) connection tests



335

336 **Fig. 6.** Load displacement curves of CLT connections with brittle layout

337



338

339 **Fig. 7.** Hysteresis curves of CLT connections

340



(a)

(b)

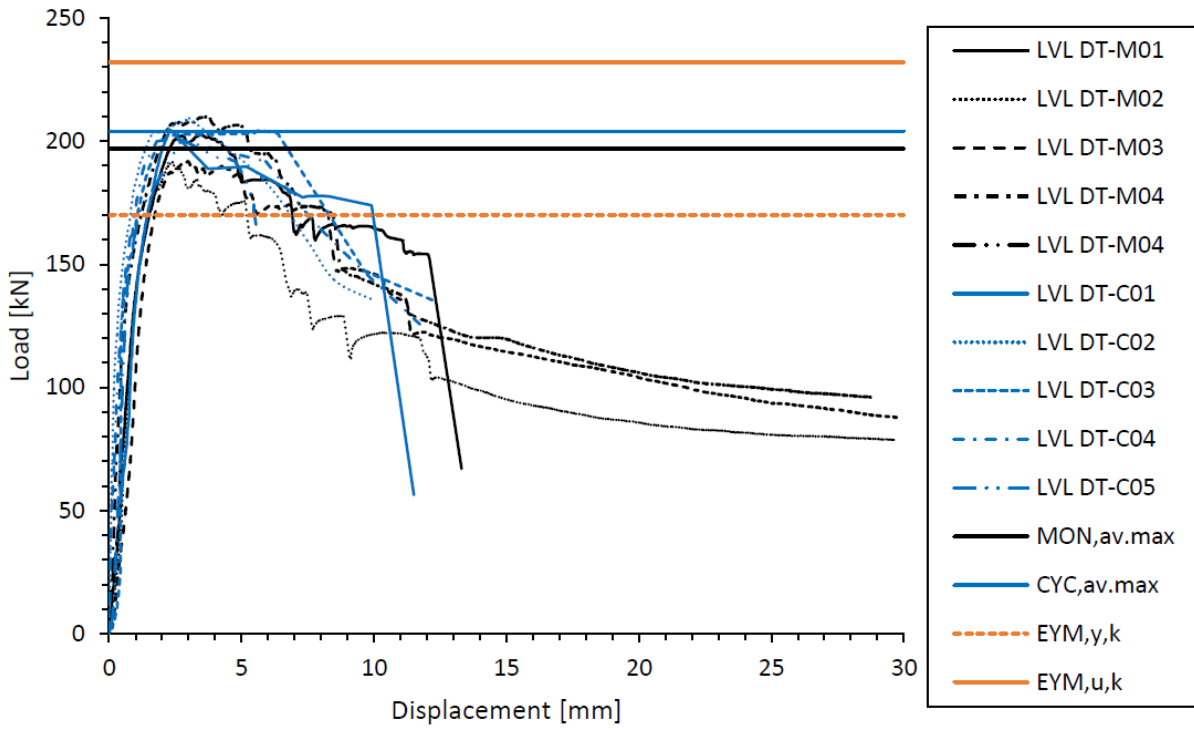
(c)

341

342 **Fig. 8.** LVL failure: (a) Row shear in DT-C and (b) RS layout, (c) group tear-out in GT layout

343

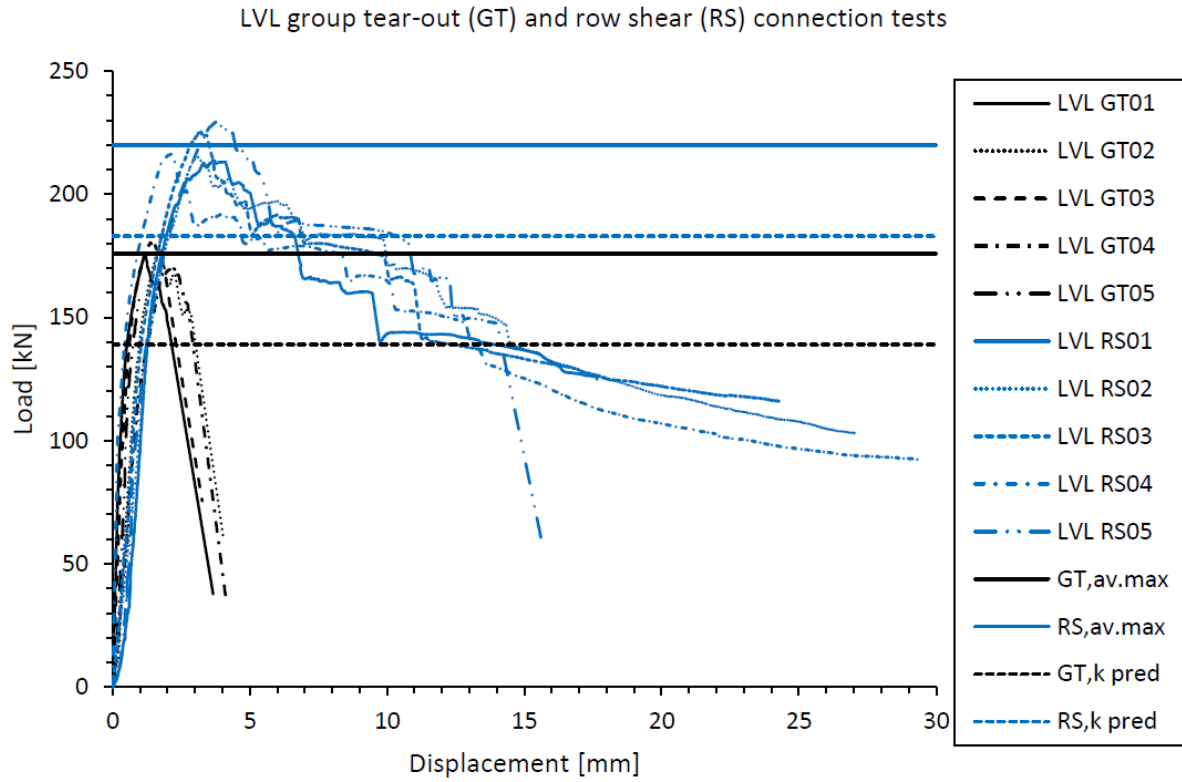
LVL ductile monotonic (DT-M) and cyclic (DT-C) connection tests



344

345 **Fig. 9.** Load displacement curves of LVL connections with ductile layout

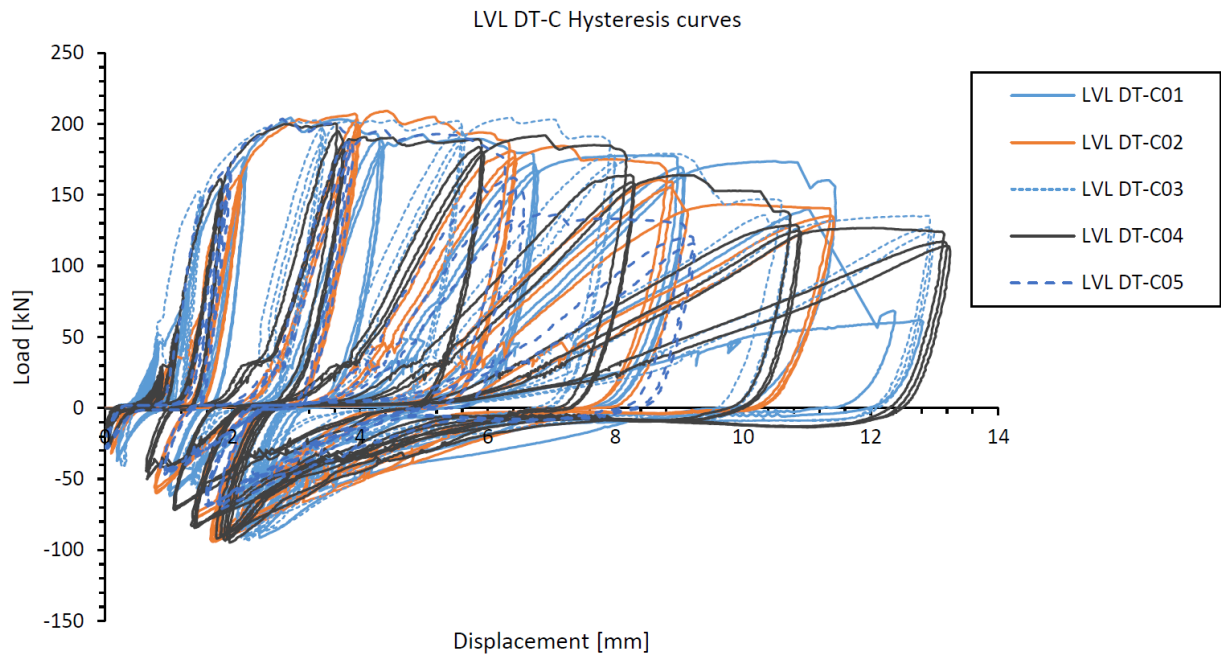
346



347

348 **Fig. 10.** Load displacement curves of LVL connections with brittle layout

349



350

351 **Fig. 11.** Hysteresis curves of LVL connections

352

353 **TABLES**354 **Table 1.** Specimen layout

	Experimental layout				Design recommendations	
	Ductile layout		Brittle layouts		LVL	CLT
	DT-M / DT-C	RS	GT-CLT	GT-LVL	Eurocode 5	Handbook
$a_1$ [mm]	100/5 <i>d</i>	80/4 <i>d</i>	80/4 <i>d</i>	80/4 <i>d</i>	5 <i>d</i>	4 <i>d</i>
$a_2$ [mm]	60/3 <i>d</i>	60/3 <i>d</i>	40/2 <i>d</i>	30/1.5 <i>d</i>	3 <i>d</i>	4 <i>d</i>
$a_3$ [mm]	100/5 <i>d</i>	140/7 <i>d</i>	140/7 <i>d</i>	140/7 <i>d</i>	7 <i>d</i>	5 <i>d</i>
$a_4$ [mm]	90/4.5 <i>d</i>	90/4.5 <i>d</i>	100/5 <i>d</i>	105/5.25 <i>d</i>	3 <i>d</i>	3 <i>d</i>

355

356

357

358 **Table 2.** Characteristic strength properties for connection strength predictions

	$f_{v,k}$ [MPa]	$f_{t,k}$ [MPa]	$f_{h,y,k}$ [MPa]	$f_{h,u,k}$ [MPa]	$M_{y,p}$ [Nmm]	$M_{y,e}$ [Nmm]
LVL	5.30	33.00	32.50	40.63	428,700	252,525
CLT	3.80	8.80	20.85	26.06	428,700	252,525

359

360

361

362 **Table 3.** Strength predictions of connections with different layouts (DT-M: ductile monotonic,  
363 DT-C: ductile cyclic, RS: row shear layout, GT: group tear-out layout, NA: not available,  
364 governing mode printed in bold)

Force [kN]	CLT			LVL		
	DT-M / DT-C	RS	GT	DT-M / DT-C	RS	GT
$F_{EYMy,k}$	124	124	124	170	170	170
$F_{EYMu,k}$	<b>174</b>	174	174	<b>232</b>	232	232
$F_{RSu,k}$	NA	NA	NA	235	<b>183</b>	183
$F_{GTu,k}$	NA	NA	NA	306	280	<b>139</b>

365

366

367 **Table 4.** CLT DT layout test results (av. = average)

CLT	DT-M (ductile monotonic)						DT-C (ductile cyclic)					
test number	1	2	3	4	5	av.	1	2	3	4	5	av.
$F_y$ [kN]	117	142	135	137	124	131	121	125	120	124	134	125
$F_{max}$ [kN]	195	178	194	198	124	178	193	195	159	171	162	176
$F_u$ [kN]	156	178	155	198	99	157	154	156	127	137	130	141
$\Delta_y$ [mm]	0.6	1.2	1.1	0.9	0.7	0.9	0.9	0.6	0.5	0.9	1.0	0.8
$\Delta_{F_{max}}$ [mm]	9.5	3.7	8.2	4.8	0.7	5.4	8.5	5.1	2.0	7.5	2.4	5.1
$\Delta_u$ [mm]	10.9	3.7	8.5	4.8	0.8	5.7	9.2	5.9	2.4	7.9	3.0	5.7
$K$ [kN/mm]	202	121	125	157	177	157	138	211	241	134	176	180
mode	D	B	D	M	B	M	D	D	M	D	M	D
$\mu = \Delta_u / \Delta_y$	18.8	3.2	7.8	5.5	1.1	7.3	10.5	10.0	4.7	8.6	8.2	8.4

368

369

370 **Table 5.** CLT GT and RS layout test results (av. = average)

CLT	GT (group tear-out)						RS (row shear)					
test number	1	2	3	4	5	av.	1	2	3	4	5	av.
$F_y$ [kN]	123	106	106	119	130	117	125	117	129	120	122	123
$F_{max}$ [kN]	175	168	164	187	186	176	224	203	136	194	134	178
$F_u$ [kN]	140	168	131	149	149	147	179	163	109	155	107	143
$\Delta_y$ [mm]	1.2	0.5	0.6	0.8	1.2	0.9	0.9	1.0	1.2	0.8	0.9	0.9
$\Delta_{F_{max}}$ [mm]	6.3	4.9	4.6	6.7	7.7	6.0	19.5	14.7	1.5	18.6	2.3	11.3
$\Delta_u$ [mm]	6.9	4.9	5.4	7.6	14.9	7.9	22.6	17.3	1.7	19.7	3.0	12.9
$K$ [kN/mm]	103	197	186	145	111	148	136	120	108	158	139	132
mode	M	D	D	D	D	D	D	D	B	D	B	D
$\mu = \Delta_u / \Delta_y$	5.8	9.0	9.4	9.3	12.6	9.2	24.6	17.7	1.4	25.9	3.4	14.6

371

372

373 **Table 6.** LVL DT layout test results (av. = average)

LVL	DT-M (ductile monotonic)						DT-C (ductile cyclic)					
test number	1	2	3	4	5	av.	1	2	3	4	5	av.
$F_y$ [kN]	184	163	184	159	178	173	163	167	130	178	158	159
$F_{max}$ [kN]	203	192	192	210	190	197	205	209	204	200	201	204
$F_u$ [kN]	162	153	153	168	152	158	164	167	164	160	161	163
$\Delta_y$ [mm]	1.3	1.1	1.7	0.9	1.3	1.2	1.2	0.9	0.6	0.9	0.8	0.8
$\Delta_{F_{max}}$ [mm]	3.5	2.4	3.0	3.8	2.2	3.0	2.1	3.0	5.7	2.6	2.0	3.1
$\Delta_u$ [mm]	7.0	6.5	8.5	8.5	6.3	7.4	10.5	7.4	8.7	7.3	5.5	7.9
$K$ [kN/mm]	142	148	108	186	137	144	141	196	232	198	211	196
mode	M	M	M	D	M	M	D	D	D	D	D	D
$\mu = \Delta_u / \Delta_y$	5.5	5.9	5.0	10.0	4.9	6.2	9.1	8.7	15.5	8.1	7.3	9.8

374

375

376 **Table 7.** LVL GT and RS layout test results (av. = average)

LVL	GT (group tear-out)						RS (row shear)					
test number	1	2	3	4	5	av.	1	2	3	4	5	av.
$F_y$ [kN]	176	151	174	154	155	162	181	196	186	145	155	160
$F_{max}$ [kN]	176	180	181	170	172	176	214	215	225	216	229	220
$F_u$ [kN]	141	144	145	136	138	140	171	172	180	173	184	176
$\Delta_y$ [mm]	1.2	0.9	1.6	1.2	0.8	1.1	1.6	1.9	1.4	0.6	0.8	1.1
$\Delta_{F_{max}}$ [mm]	1.2	1.7	2.0	2.2	1.7	1.8	3.7	3.0	3.2	2.1	3.5	3.8
$\Delta_u$ [mm]	2.1	3.0	2.8	3.1	2.4	2.7	6.9	10.0	7.0	7.5	9.9	8.3
$K$ [kN/mm]	147	168	109	128	194	149	112	104	136	242	194	157
mode	B	B	B	B	B	B	M	M	M	D	D	M
$\mu = \Delta_u / \Delta_y$	1.8	3.3	1.7	2.5	3.0	2.5	4.3	5.3	5.1	12.5	12.4	7.9

377

378

379 **Table 8.** Average ductility and ultimate displacement of connection tests

	CLT				LVL			
	DT-M	DT-C	GT	RS	DT-M	DT-C	GT	RS
$\mu_{av}$ [-]	7.3	8.4	9.2	14.6	6.2	9.8	2.5	7.9
$\Delta_{u,av}$ [mm]	5.7	5.7	7.9	12.9	7.4	7.9	2.7	8.3
average mode	M	D	D	D	M	D	B	M

380

381

382 **Table 9.** Comparison of strength prediction with experimental results

		CLT		LVL	
		average	predicted	average	predicted
		maximum	characteristic	maximum	characteristic
DT-M	$F_y$ [kN]	131	124	173	170
	$F_{max}$ [kN]	178	174	197	216
DT-C	$F_y$ [kN]	125	124	159	170
	$F_{max}$ [kN]	176	174	204	216
GT	$F_y$ [kN]	117	124	162	170
	$F_{max}$ [kN]	176	-	176	139
RS	$F_y$ [kN]	123	124	172	170
	$F_{max}$ [kN]	178	-	220	183

383

384

## 386 NOTATIONS

$CYC_{av.max}$	cyclic average maximum strength
$DT$	ductile layout designation or strength
$F_{BRred}$	reduced brittle connection strength
$F_{BRu}$	ultimate brittle connection strength
$F_d$	design strength
$F_{EYMu}$	ultimate ductile connection strength based on European Yield Model
$F_{EYMy}$	connection's yield strength based on European Yield Model
$F_{GT}$	group tear-out strength
$F_k$	characteristic strength
$F_{max}$	connection's peak strength
$F_{RS}$	row shear strength
$F_u$	connection's ultimate strength
$F_y$	connection's yield strength / yield point
$GT_{av.max}$	group tear-out layout average maximum strength
$K$	initial stiffness
$k_{LS}$	loading surface factor (0.65 for internal steel plate)
$M_{y,e}$	fastener's elastic yield moment
$M_{y,p}$	fastener's plastic yield moment
$MON_{av.max}$	monotonic average maximum strength
$RS_{av.max}$	row shear layout average maximum strength

$a_1$	fastener spacing in row
$a_2$	fastener spacing between rows
$a_3$	edge distance in to loaded edge
$a_4$	edge distance to unloaded edge
$d$	fastener diameter
$f_{h,u}$	ultimate embedment strength
$f_{h,y}$	yield embedment strength
$f_t$	tensile strength
$f_u$	fastener ultimate tensile strength
$f_v$	shear strength
$f_y$	fastener yield strength
$t_1$	single side timber member thickness

388

$\alpha_1$	row shear calibration factor (0.84)
$\alpha_2$	group tear-out calibration factor (1.26)
$\Delta_{Fmax}$	displacement at peak load
$\Delta_u$	ultimate displacement / displacement at 80% of the maximum load
$\Delta_y$	yield displacement
$\mu$	ductility
$\rho$	timber density

389

390 **REFERENCES**

- 391 • American Society for Testing and Materials, ASTM D5764-97a (2013). “Standard Test  
392 Method for Evaluating Dowel-Bearing Strength of Wood and Wood-Based Products.  
393 Standard test method for evaluating dowel- bearing strength of wood and wood-base  
394 products”. *ASTM International*, West Conshohocken, PA.
- 395 • Australian/New Zealand Standard, AS/NZS 4357.0:2005 (2005). “Structural Laminated  
396 Veneer Lumber.” *Standards Australia*, GPO Box 476, Sydney, NSW 2001 and *Standards*  
397 *New Zealand*, Wellington 6140.
- 398 • Australian/New Zealand Standard, AS/NZS 4671:2001 (2001). “Steel reinforcing  
399 materials (2001).” *Standards Australia*, GPO Box 476, Sydney, NSW 2001 and *Standards*  
400 *New Zealand*, Private Bag 2439, Wellington 6140.
- 401 • Australian/New Zealand Standard, AS/NZS ISO 10984.1:2015 (2015). “Timber structures  
402 - Dowel-type fasteners - Determination of yield moment” (2015). *Standards Australia*,  
403 GPO Box 476, Sydney, NSW 2001 and *Standards New Zealand*, Private Bag 2439,  
404 Wellington 6140.
- 405 • Australian/New Zealand Standard, AS/NZS ISO 10984.2:2015 (2015). “Timber structures  
406 - Dowel-type fasteners - Determination of embedding strength” (2015). *Standards*  
407 *Australia*, GPO Box 476, Sydney, NSW 2001 and *Standards New Zealand*, Private Bag  
408 2439, Wellington 6140.
- 409 • Brühl, F., Kuhlmann, U., Jorissen, A. (2011). “Consideration of plasticity within the design  
410 of timber structures due to connection ductility.” *Engineering Structures*, 33(11), 3007–  
411 3017.

- 412 • European Standard EN 1995-1-1 2004/A1 2008 Eurocode 5 (2004/2008). “Design of  
413 timber structures - part 1-1: general- common rules and rules for buildings/incl Amendment  
414 A1.” *European Committee for Standardization*, Bruxelles (Belgium).
- 415 • European Standard EN 12512 (2013): “Timber structures - Test methods - Cyclic testing  
416 of joints made with mechanical fasteners.” *European Committee for Standardization*  
417 (CEN), Bruxelles. (2013)
- 418 • Flatscher, G. (2016). "Evaluation and approximation of timber connection properties for  
419 displacement-based simulation of CLT wall systems (working title)", Doctoral thesis, Graz  
420 University of Technology, Austria
- 421 • Franke, S., Quenneville, P. (2011). “Bolted and dowelled connections in radiate pine and  
422 laminated veneer lumber using the European yield model.” *Australian Journal of*  
423 *Structural Engineering*, 12(1), 13–28.
- 424 • International Organization for Standardization ISO 16670:2003 (2003). “Timber structures  
425 – Joints made with mechanical fasteners – Quasi-static reversed-cyclic test method  
426 (2003).” *The international Organization for Standardization*, Geneva.
- 427 • Jensen, J. L., & Quenneville, P. (2011). Experimental investigations on row shear and  
428 splitting in bolted connections. *Construction and Building Materials*, 25(5), 2420–2425.
- 429 • Jorissen, A., Fragiacom, M. (2011). “General notes on ductility in timber structures.”  
430 *Engineering Structures*, 33(11), 2987–2997.
- 431 • Karacabeyli, E., Desjardins, R. Eds (2011). “CLT Handbook.” *FPInnovations*.
- 432 • Mohammad, M., Quenneville, J. H. P., Smith, I. (1998). “Influence of cyclic loads on  
433 strength and stiffness of bolted timber connections.” *Proceedings of the 5th World*  
434 *Conference on Timber Engineering* Vol. 1, pp. 375-382.

- 435 • Moroder, D., Smith, T., Pampanin, S., Palermo, A., Buchanan, A. H. (2014). "Design of  
436 Floor Diaphragms in Multi-Storey Timber Buildings." *Proc. INTER*, 2014.
- 437 • Novis, S. A. L., Jacks, J., & Quenneville, P. (2016). "Predicting the Resistance and  
438 Displacement of Timber Bolted Connections." In *Proceedings WCTE*, 2016.
- 439 • Ottenhaus, L.M., Li, M., Smith, T., & Quenneville, P. (2016). "Ductility and Overstrength  
440 of Dowelled LVL and CLT Connections Under Cyclic Loading." In *Proceedings WCTE*,  
441 2016.
- 442 • Ottenhaus, L.-M., Li, M., Smith, T., & Quenneville, P. (2017). Overstrength of dowelled  
443 CLT connections under monotonic and cyclic loading. *Bulletin of Earthquake*  
444 *Engineering*.
- 445 • Piazza, M., Polastri, A., Tomasi, R. (2011). "Ductility of timber joints under static and  
446 cyclic loads." *Proceedings of the ICE - Structures and Buildings*, 164(2), 79–90.
- 447 • Quenneville, P., & Morris, H. (2009). "Proposal for a mechanics-based bolted connection  
448 design approach for AS1720.1." *Australian Journal of Structural Engineering*, 9(3), 195–  
449 206.
- 450 • Smith, I., Asiz, A., Snow, M., Chui, Y. H. (2006). "Possible Canadian / ISO Approach to  
451 Deriving Design Values from Test Data." *CIB W18 Meeting Thirty-Nine*, Florence,  
452 (August).
- 453 • Smith, T., Moroder, D., Sarti, F., Pampanin, S., Buchanan, A.H. (2015). "The Reality of  
454 Seismic Engineering in a Modern Timber World." *Proc. INTER*, 2015.
- 455 • Yasumura, M. "Mechanical properties of dowel type joints under reversed cyclic lateral  
456 loading." *Proceedings CIB-W18-meeting*. Savonlinna, Finland. Universität Karlsruhe, CIB  
457 W. Vol. 18. 1998.

- 458       • Zhang, Y., Raftery, G. M., Quenneville, P. (2016). "Predicting the Load-Deformation of  
459       Bolted Timber Connections up to Failure." *Proc. INTER 2016*, Graz  
460  
461